

## Effect of Substrate Temperatures based green synthesized silver thin films prepared by the spray pyrolysis of FTO conducting glass and Dye sensitized solar cells

K. Ramya<sup>1</sup>, S.Ravi<sup>2</sup> and G.suresh<sup>3</sup>

<sup>1</sup> Department of Physics, Annamalai University, Annamalai Nagar – 608002, TamilNadu, India

<sup>2</sup> Department of Engineering Physics (FEAT), Annamalai University, Annamalai Nagar- 608 002, India

<sup>3</sup> Department of physics (Directorate of Distance Education) Annamalai University, Annamalai Nagar - 608 002, India.

ramya.nethra2015@gmail.com,

### Abstract

In the current work, thin films of nano structured silver were prepared with different substrate temperatures from Spray pyrolysis technique. DSSC was significantly by green-synthesized silver thin-films. Silver through treating metallic ions with silver ions, Vitex negundo leaf extract at room temperature. The Transparent Conductive Oxide (TCO) constituents of the Dye Sensitized Solar Cell (DSSC), a system built as a source of renewable energy with high potential. TCO glasses of Fluorine-Doped Tin Oxide (FTO) has the highest development. The purpose of this research is to find an optimum temperature of the substrate during the process of spray pyrolysis to obtain the desired FTO substrates. This reason, beakers were deposited with a mixture of precursors using a specially modified nebulizer and digital multimeter of substrate heating temperatures 100,150,200 and 250°C. All produced samples were characterized by UV-vis and Photoluminescence [PL], Field Emission Scanning Electron Microscope [FE-SEM] with Energy Dispersive X-Ray Spectroscopy [EDX], X-Ray Diffraction [XRD] and Atomic Force Microscopy [AFM]. Finally, solar cell shows low to high temperatures in silver of DSSC.

**Keywords;** Green synthesis, silver, FTO glass plate and XRD.

### 1. INTRODUCTION

Thin film-based solar cells seem to be an eminent technology for stable cells production. Due to their low resistance and high optical absorption, Transparent Conductive Oxide (TCO) thin films have attracted a lot of attention and have been widely used in a wide range of applications, including architectural windows, cells solar cells, and thermal reinforcements, transparent and electrodes. [1]. Over the past decade processes and new materials for dye sensitive solar cells (DSSC) have been thoroughly researched to improve cell performance and stability [2]. Dyes sensitive Solar cell (DSSC), a third generation solar cell was first residential the Gratzal group its collaborators [3]. DSSC has fascinated an important consideration because of its low production cost, ease of assembly and respect for the environment. Dyes sensitizer together with electrolyte and counter electrodes, the first to produces a DSSC [4]. Since the discovery of DSSC, many new approaches have been developed to obtain high-performance DSSC with modification of metal photodiode materials with control electrode, electrolyte, dye and Nobel. We chose the noble silver metal because its observance band coincides with the low energy dye band. This article tries to synthesize the Ag thin film through the green path. The green synthesizer is effective not only for synthesizing noble metals [5]. The one of the most favorable photovoltaic cells is the DSSC. This device consists of many imperative components, with the usual Transparent Conductive Oxide (TCO), produced coating

and retaining clarity of the conductive portion of the glass substrate. One of the most prospective photovoltaic cells is the Dye Sensitized Solar Cell. This device consists of a variety of Main components, including transparent conductive oxide (TCO) [6]. Element of conductive oxide for its good electrical properties and its high availability on earth. For a good TCO criterion, electrical properties alone are not adequate, as they must also have good clarity to allow the Sunlight photon energy to be passed to the DSSC device within and thus both excite the electrons in the semiconductor oxide layer [7]. Toward obtain optimum value, the inclusion of the doping factor helps preserve the equilibrium between the two properties. Indium-doped tin oxide (ITO) is also used for most solar cells as TCO. However, while the outcome is satisfactory, indium is quite an unusual and hazardous method as a doping element. This is the beginning of several works to substitute the Indian with another doping factor. To achieve optimum characteristics for TCO, different conductive elements such as doping have been tested [8]. While the outcome has been very positive, owing to its strong consumer demand, it is still hard to make it economically viable. Fluorine (F) is the most promising possible candidate. In addition to its ample supply of land, processing it on a large scale is also safe. The film of Different techniques by sputtering [9], spray pyrolysis [10], immersion coating [11] and chemical vapour deposition [12] were used to prepare Fluorine-Doped Tin Oxide (FTO) by rotation [13]. Among these techniques, it was thought that spray pyrolysis is the most versatile due to simplicity and low operating costs allowing controlled in FTO substrate temperatures [14].

### **In this present study,**

effect of the heating temperature of substrate varies at (100, 150, 200 and 250°C) through the use of thin Ag films synthesized in green. Characteristics of the manufactured FTO conductive glass in there; morphologies, crystalline structure, and optical absorption through the use of with a specially adapted nebulizer, a basic spray pyrolysis technique. The absorption spectra of natural dye extracts and the thin films absorbed by the *Vitex negundo* leaf are discussed. In addition to the performance of the DSSC produced using dye extracts as a sensitizer the calculation of J-V and the normal value used for the computation are analyzed.

## **2. EXPERIMENTAL SETUP**

### **2.1 Materials and Methods**

Silver nitrate ( $\text{AgNO}_3$ ) 98%, FTO plate L×W×thickness, 300mm × 300 mm × 3 mm, surface resistivity  $\sim 10\Omega/\text{sq.}$ , silver paste. Analytical purity of chemical reagents was purchased from Merck. The dye resultant from the solution. The natural extracts solution used. All the glassware be cleaned with acetone follow by a complete washing among distilled water, deionized water was used a complete experiments.

### **2.2 For the preparation of leaf extracts**

A photograph of fresh leaves from the garden of the Department of Agriculture, Annamalai University and Chidambaram obtained from the *Vitex negundo* leaf. Fresh leaves were thoroughly rinsed with deionized water for the preparation of the leaf extract. They cut 10 g of *Vitex negundo* leaves into small pieces. In 100 ml of deionized water, the chopped leaves were boiled for 10 minutes. The leaf extract was then cooled through the filter paper and filtered (What man No. 1). The colour and translucency of the extract comprising the bottle of leaves.

### 2.3 Preparation of the substrate and material

FTO Substrates were 2.5 x 1.5 cm glass one of the controls was cut to spot the pyrolysis region sprayed. They were washed with soap for the first time in order to extract clay also put for 30 minutes in a nitric acid-containing beaker. The washed before being used for thin film, substrates were then dried overnight in the oven processing.

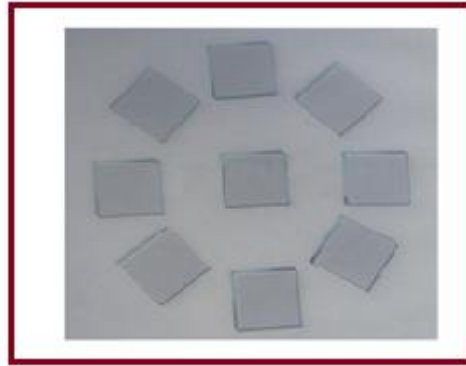
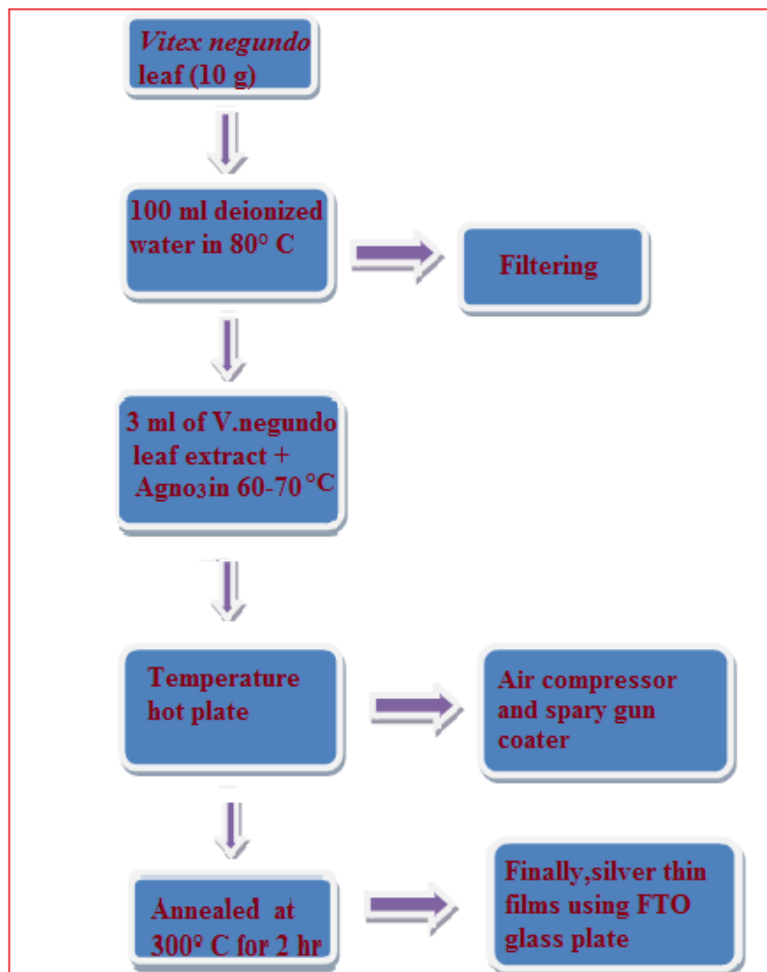


Figure: 1 FTO substrates 2.5×1.5 cm

### 2.4 Preparation of silver thin films

Experimental setup for depositing thin silver films on the substrate of FTO glass. By mixing equivalent amounts of 1 mM silver nitrate solution ( $\text{AgNO}_3$ ) and 10 g of *Vitex negundo* leaf extract, the chemical bath was produced. The substrates were preheated for a particular duration before rendering the deposition and then the synthesized solvent was sprayed, respectively. Decomposition process occurs when the precursor aerosol droplets pass near the heated substrate and, subsequently high-quality  $\text{AgNO}_3$  films have been created. Digital multimeter Measurement in the conductive material of the FTO glass plate. The pyrolysis spray was carried out for 20 minutes at a heating temperature of different substrates of 100, 150, 200 and 250°C. Subsequently, the films deposited were allowed to cool slowly for 2 hours at room temperature, dried and then calcinated 250°C. Finally, the deposited thin films are characterized.



**Flowchart for the preparation of silver thin film using FTO glass plate**

### Characterization technique used

X-Ray Diffraction techniques using SHIMADZU-6000 fitted with monochromatic Cu-K $\alpha$  radiation ( $\lambda = 1.5406 \text{ \AA}$ ) used to structurally classify the deposited films. Using the JEOL 6300 field emission scanning electron microscope, the surface morphology was analyzed (FESEM). The JASCO V-670 spectrometer; optical absorption spectra were recorded within the 300-1200 nm range. At room temperature, photoluminescence (PL) spectra have been reported. The topological analysis Atomic Force Microscopy (AFM) was conducted using AGILENT-N9410A-5500 (Nano Surf Simple Scan 2). Using a solar energy meter under lighting conditions, JV measurements were made with a light source capable of providing solar radiation equivalent to  $1000 \text{ W} \cdot \text{m}^{-2}$  (AM 1.5), using the photovoltaic cell energy meter under lighting conditions.

### 3. RESULTS AND DISCUSSION

#### 3.1 Structural study

The diffractogram for FTO thin films made with thin films shown in Figure 3.1 heating temperatures of 100, 150, 200 and 250 ° C for the substrate. Ag thin film XRD versions synthesized in green from *Vitex negundo* leaf extract [15]. As the temperatures heating substrate improved to 250°C crystallinity FTO sample was developed, as seen by exhibition of four major Peaks of characteristic diffraction for Ag with a 2θ angle of 38.2, 44.4, 64.5 and 77.5 corresponding crystalline plane values (111), (200), (220) and (311) similarly. The findings attained are in strong alignment with the **JCPDS card No. 89-3722** reference models affirm crystalline existence the Face-Centered Cubic structure (FCC) of Ag thin films prepared. [16]. It can be shown that the sample was still crystalline at 100, 150, 200 and 250°C, as shown by the statement that the diffusion peaks had not however emerged. Current crystal planes, (111) as represented by its high crystallinity, given the highest peak. It is important to note that this peak has raised the glass even further with the increase in the heating temperature of the layer to 250°C leading to the rise the film temperatures. [17]. A more increase the temperature of the substrate up 250°C cause decrease in the crystal planes, while the plan (200) was maintained, but its intensity decreased considerably. The mainly evident high intensity peak was provided only by the aircraft (111) in this sampling condition. Similar phenomena have been report that at a substrate temperature 250°C, low intensity peak have faded due evaporation of Ag thin film, leaving the plane (111) to become the strongest [18].

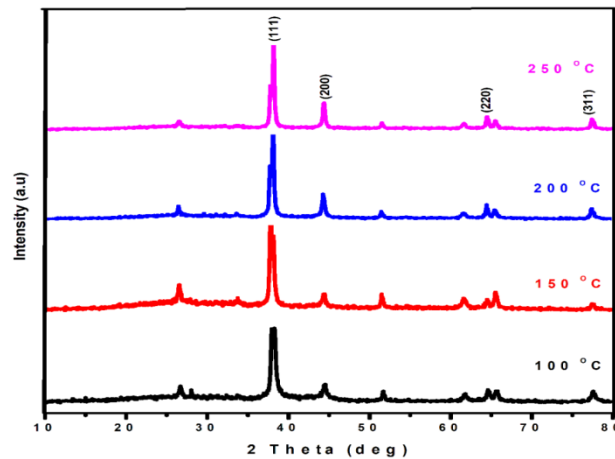


Figure 3.1. XRD spectra for silver thin films at different substrate temperatures.

#### Crystalline size (D)

Substrate temperature, crystallite size of Ag increases and is determined by Debye- Scherer’s formula.

$$D = \frac{k\lambda}{\beta \cos\theta} \text{----- (1)}$$

Where the form factor k= 0.9 the wavelength that is used is (1.5405 Å) in radians, β is half the maximum width limit FWHM, θ is the angle of Bragg. Increase in crystalline size with a decrease in strain from Table.1. The density of dislocation suggests the improved crystallinity of the prepared films at 250°C. As seen in Fig. 1,

the rise in crystalline size and dislocation density with reduction strain for the film which was deposited at 250°C the phase transition can be attributed.

### Dislocation density ( $\delta$ )

Dislocation density ( $\delta$ ) Using the relationship ratio, meaning is calculated.

$$\delta = \frac{1}{D^2} \text{----- (2)}$$

The basic method of Williamson and Smallman describes dislocation density as the length of the lines of dislocation per volume unit of the crystals was calculated by the following relationship (pan et al., 2013).

### Strain ( $\epsilon$ )

The strain ( $\epsilon$ ) is determined using the relationship

$$\epsilon = \frac{\beta \cos \theta}{4} \text{----- (3)}$$

Where  $\beta$  in radians is FWHM,  $\theta$  is the Bragg's angle. Strain these films has been found to be reduced, which may be due to thin film crystallization. It was observed that the strain of these films was limited, which could be due to thin film crystallization.

**Table:-1** Ag thin films obtained at different substrate temperatures.

S.No	Substrate temperature (°c)	2 $\theta$ (degree)	(h k l) planes	FWHM	d - spacing	Crystalline size (D) (nm)	Dislocation density ( $\delta$ ) $\times 10^{14}$ lines/m <sup>2</sup>	Strain ( $\epsilon$ ) $\times 10^4$
1.	100	38.2500	111	0.1968	2.35307	43.2142	4.3017	0.0640
2.	150	44.4074	200	0.1181	2.04005	43.5416	4.6165	0.0417
3.	200	64.5636	220	0.1181	1.44348	45.4166	4.8480	0.0386
4.	250	77.5467	311	0.2880	1.23004	48.3338	5.3253	0.0337

### 3.2 optical properties

#### Absorption

The UV-Vis absorption spectrum of thin silver films deposited by varying substrate temperature as seen Figure 3.2. The increased absorption is due to adhesion and the stronger crystalline structure of the film that the XRD measurements create. Over 350-1200 nm of the spectral range. Absorption spectra of attained thin film of Ag. Band of absorption at around 425 nm is evidently attributed to the Ag thin film band and hence confirms the existence of Ag. The mean absorption of the film deposited at the temperature of the substrate is between 100, 150, 200 and 250°C between absorption of whole substrate temperature. The findings above agree with the outcomes stated. The higher the temperature of the layer, the lower the average absorption induced by the rise in film defects [19, 20]. And that may also be attributed to the XRD outcomes being consumed. Who discovered that with the increase of the crystal size induced by the coating, the optical absorption of the temperature of the FTO thin films increases and it could also be due to the absorption of the XRD results. Who discovered that the optical absorption of the temperatures FTO thin films increase of the crystal size caused by the coating [21].

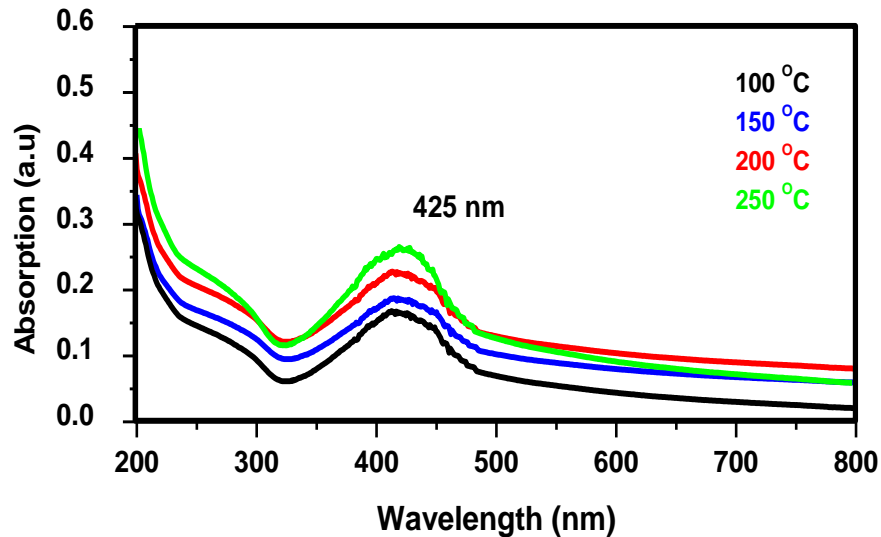


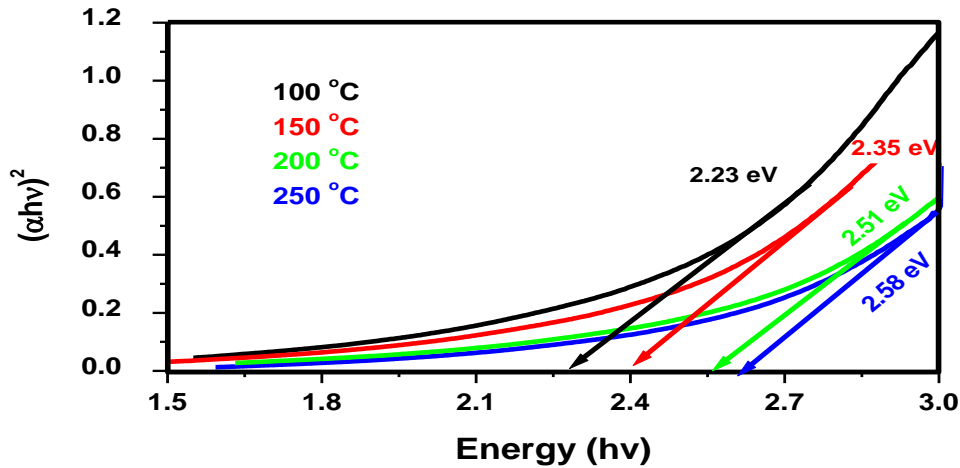
Fig 3.2. Optical absorption of the FTO glasses deposited at 100, 150, 200 and 250°C

### 3.3 Optical band gap

In the 350-1200 nm wavelength range, optical absorption spectra are recorded. The optical energy of the band gap of silver thin films at various temperatures is calculated for the directional transformation using the equation below:

$$(\alpha h\nu) = A (h\nu - E_g)^{1/2} \text{----- (4)}$$

Where  $\alpha$  is optical absorption coefficient,  $h\nu$  is the photon energy,  $A$  is a constant and  $n$  this number depends on the existence of the conversion direct and indirect transformation values of  $1/2$  and  $2$ . Space the optical band silver thin film is shown in Figure 3. The values of the space of the energy band seem to increase. Band gap values obtained from 2.23eV, 2.35 eV, 2.51eV and 2.58 eV, due to the formation of nano-sized particles [22]. The separation of the strips decreases to increasing temperatures of the film, indicating the effect of the increase in the



size of the particles, moreover, the stress of the film tends to increase with temperature, causing changes in the edges of the band.

**Figure 3.3  $(\alpha h\nu)^2$  Vs photon energy plot of the silver thin film at substrate temperatures from 100, 150, 200 and 250°C**

### 3.4 Photoluminescence (PL) spectrum study

The silver films synthesized are derived from the photoluminescence (PL) spectra seen in Figure 3.3. It is shown that the PL peak was 445 nm for all the various substrate temperatures of the silver thin films [23]. In the spectrum of wavelengths from 200 to 800 nm, PL emission peak and the visible UV peak have emerged. In the emission area of the band edge, the photoluminescence (PL) spectrum of the prepared films was studied. The intensity of PL appears in the wavelength (445nm) as that of the exciton band observed in the optical absorption spectra [24]. consequences analysis of the PL spectroscopy cultivated sections is displayed in Fig.3.4. Small variations near the region of shorter wavelength (blue displacement) are observed in the PL spectra increasing substrate temperature. The variation of substrate temperature increases is an indication of the release of localized extended state carriers. The peak change is also an indication of the existence of a surface energy level [25].

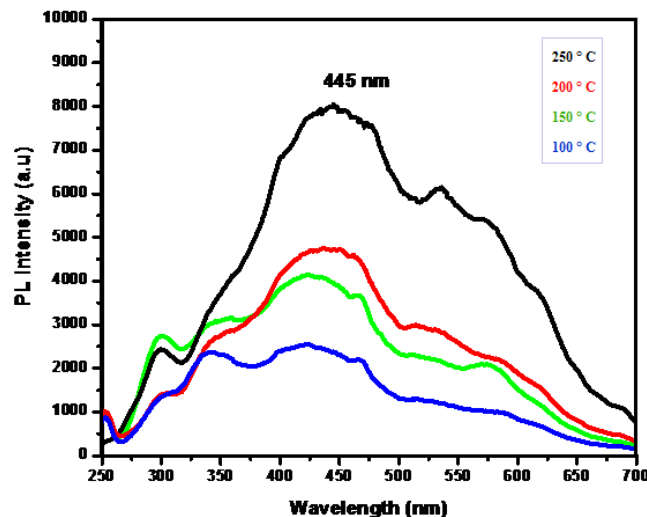
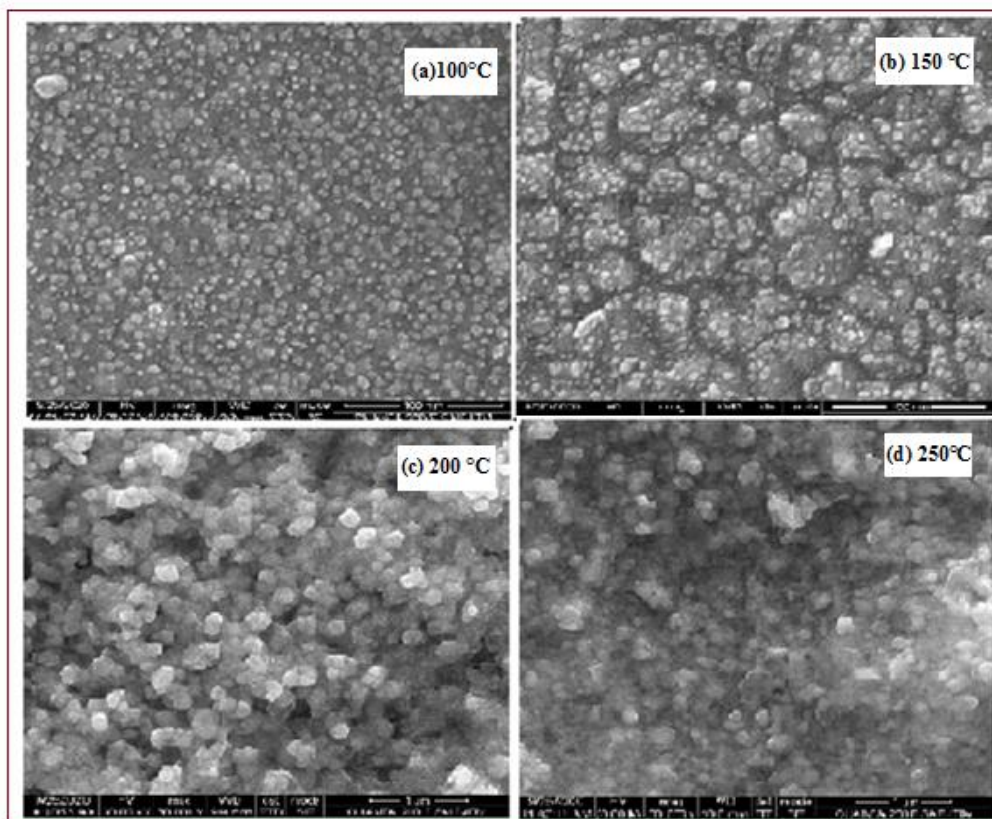


**Fig. 3.4. PL spectra of silver thin film on substrate temperatures**

### 3.5 Morphological studies

#### 3.5.1 Surface morphology

The micro structural study of the silver thin film is carried out. FESEM illustration of thin films (fig.3.5.1) on the FTO different substrate temperatures Ag-thin films respectively. FESEM images were provided. The FESEM images surface of the FTO substrates. The film deposited at 100,150,200 and 250°C indicates that temperatures increased. Size of the grains is increased and exhibits well definite grains of spherical shape [26].Surface morphology of the studied films (58 nm) by FESEM. It showed that surfaces as substrate temperature increased. At substrate temperatures, 250°C, over the entire surface clear from these images that a



Common characteristics of the thin film is spherical shape with absence of closed morphology.

**Fig.3.5.1. FE-SEM images of Ag thin films substrate temperatures**

#### 3.5.2 Elemental analysis

Analysis will be performed to check the chemical composition of the EDX film. Appearance the spectrum Ag peaks is due to the glass substrate's FTO coating. EDX spectrum clearly reveals elements such as si, ca, cl and O present the film material. EDX analysis of different substrate temperatures shows Ag films. Considered Ag spectra line become more extreme films obtained from solution with higher silver temperature 250°C [27]. The line is also important to remember. Since the EDX approach is not capable of distinguishing between elemental Ag in other compounds, this finding is only demonstrated by the rise in nano-film of Ag. The increased Ag line strength is due to the increased silver content of the nano film.

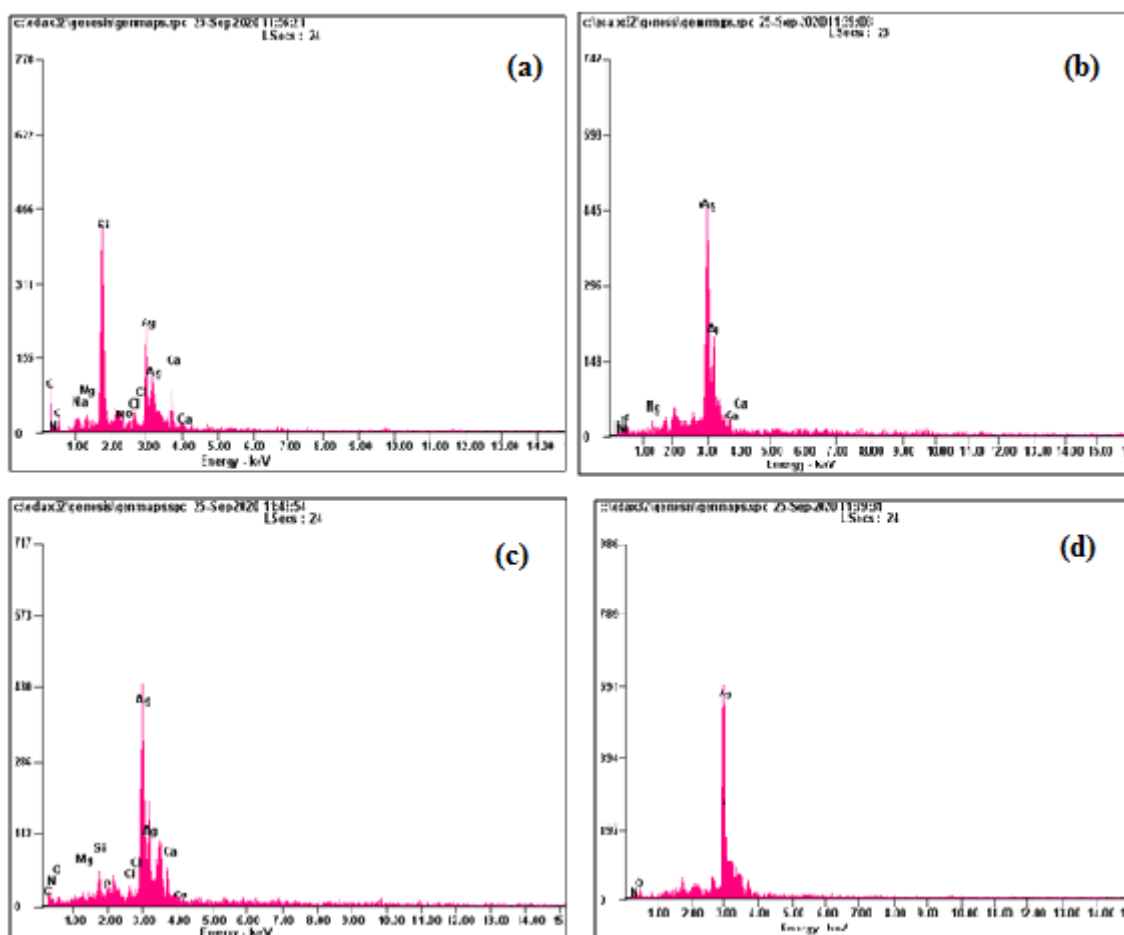


**Fig 3.5.2 Glass coated with Ag microstructures film deposited from EDX spectra. (A) 100 (B) 150 (C) 200 and (D) 250°C**

### 3.6 Surface topography

AFM analysis surface roughness of as deposited and substrate temperature Ag thin films. Top- (2D) and - (3D) view images in Figure 3.6 illustrate the surface morphologies of a  $3 \times 3\text{-}\mu\text{m}^2$  area of the temperature silver films. At 100 and 250°C have more surface roughness ( $R_a$ ) due to the presence of a crystalline film [28]. However, Substrate temperatures increased. Surface roughness notably increased due to increased crystal size as observed

correlate with the microstructure of Ag NPs thin films by (XRD).The surface roughness of the film deposited at 250 °C helps to enhance the wide surface area that the solar cell may need.

Table 2 shows that for all Ag temperature films, the variations in the values of arithmetic mean height ( $R_a$ ), root mean square roughness ( $R_q$ ), total peak height ( $R_z$ ), maximum height ( $R_z$ ) and Skewness ( $R_{sk}$ ) and kurtosis ( $R_{ku}$ )-Average characteristics in the height direction. A very important parameter is also considered to be Maximum peak to valley ( $R_t$ ) height since it provides a clear overview of the overall roughness of the surface.

$$R_z = \frac{1}{n}(\sum_{i=1}^n P_i - \sum_{i=1}^n V_i) \quad \text{----- (5)}$$

Where  $R_z$  is Also strong, owing to the heavy dependency of  $R_z$  on mountain Heights/depths of the valley. $n$  is the number of sampling points over the range of the assessment,  $P_i$  is the peak height of the  $i^{th}$  peak and  $V_i$  is the line profile depth. Furthermore,  $R_q$  values are higher than  $R_a$  values for all samples, which can be explained mathematically according to the following equation:

$$R_z = \frac{1}{L} \int_0^L [y(x)]. dx \quad \text{----- (6)}$$

$$R_q = \sqrt{\frac{1}{L} \int_0^L [(y(x))^2]. dx} \quad \text{----- (7)}$$

Where the length of is  $L$  x-axis outline used for measuring,  $y(x)$  is the height change for each data point from the profile line.

According to the following formula,  $R_{ku}$  is explicitly related mathematically to peak heights and valley depths:

$$R_{ku} = \frac{1}{NR_q^4}(\sum_{i=1}^N Y_i^4) \quad \text{----- (8)}$$

**Table: 2. Roughness parameters of silver thin film substrate temperatures**

Substrate Temperature (°C)	$R_a$ nm	$R_q$ nm	$R_t$ nm	$R_z$ nm	$R_q/R_a$	$R_{sk}$	$R_{ku}$
100	8.04	10.0	39.1	72.5	1.243	0.089	2.98
150	17.7	15.7	76.7	138	0.887	0.233	2.96
200	20.3	21.8	82.1	139	1.073	0.565	3.95
250	23.2	29.4	111	229	1.267	0.169	3.50

Films with high  $R_{ku}$  values also have high  $R_t$  and  $R_z$  values in temperatures of 100, 150, 200 and 250°C. This is due to these parameters being closely related.

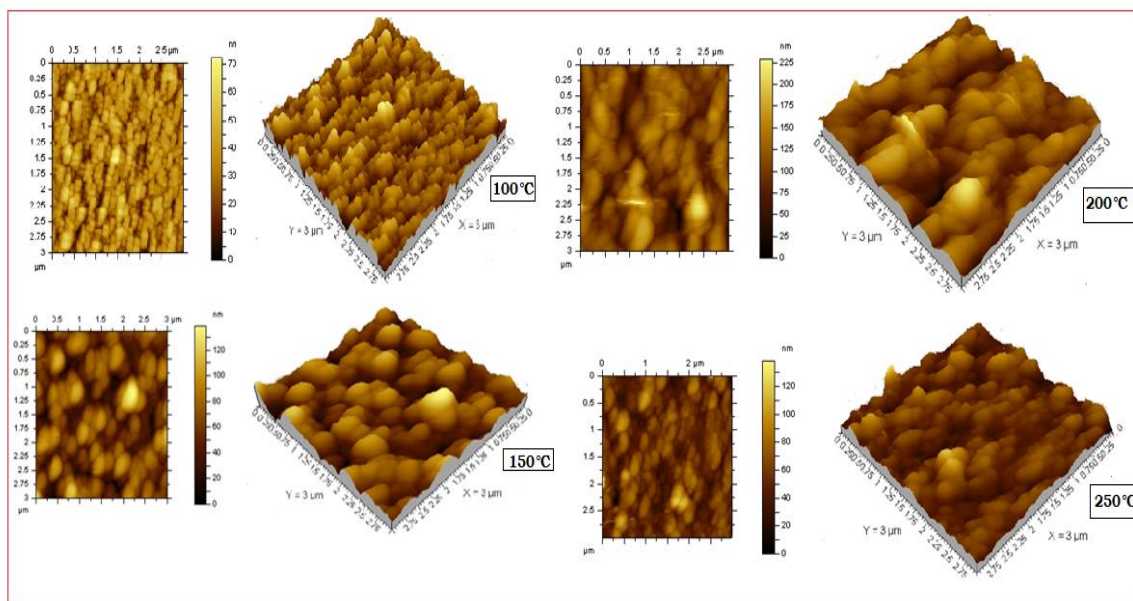


Fig. 3.6 AFM (2D and 3D) images of Ag films at different substrate temperatures

### 3.7 Photovoltaic characterization

The green synthesis of thin silver films and the growth of DSSC. There are however, very few studies on system manufacturing so far comprising DSSCs spending green synthesized thin Ag films. In this study, the DSSC green synthesized silver thin film this technology decreases the non-toxic use of DSSC production process.

J/V characteristics of Ag thin films by 100, 150, 200 and 250°C substrate temperatures of Ag thin films stayed evaluated values of the DSSC. Figure 3.5 shows the characteristics of the DSSC's photocurrent voltage (J-V) prepared with silver on an FTO glass plates substrate placed as electrolyte at dissimilar substrate temperatures. Using the dye extracted from *Vitex negundo*, the solar cell performance parameters are manufactured with the Ag. From the data it is clear that with the application of dye as a sensitizer, *Vitex negundo* with Ag- the best output is given by the base cell.

Injected electrons flow towards the counter electrode through the external charge, where they regenerate the dye with the reduction. Therefore, collected light is transformed into electricity [29]. When the sunlight enters the solar cell, the dye sensitizers on the silver film surface get excited and the electrons are pumped into the solar cell. Ag in turn. Inside the Ag film, the electrons injected spread all the way through the film to the external load used to do useful work. Finally, the electrolyte in the counter electrode captures these electrons to complete the loop, which is absorbed to regenerate the dye sensitizer in turn. The overall performance of the DSSC can be measured based on sunlight-to-electric power conversion quality.

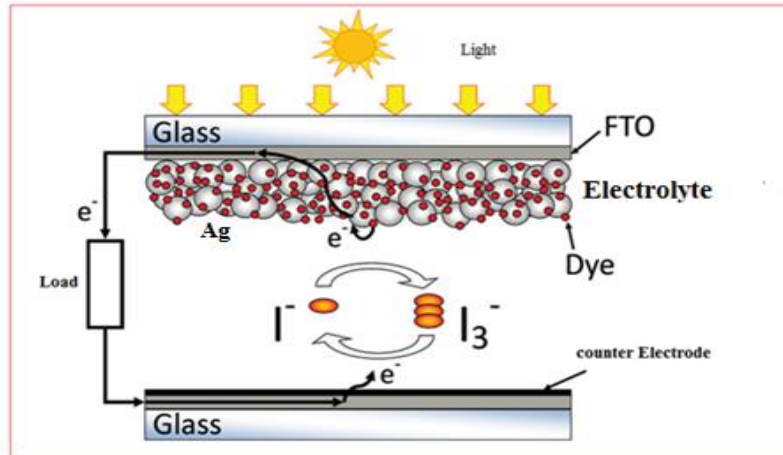


Figure (a).3.7 DSSC solar cells

The Measured current density at short circuit ( $J_{sc}$ ), open circuit voltage ( $V_{oc}$ ), Fill Factor (FF), intensity light ( $P_{in}$ ) For a photovoltaic cell energy conversion efficiency ( $\eta$ ), as defined by following expression:

$$\eta = \frac{J_{sc} V_{oc} FF}{P_{in}} \quad \text{----- (9)}$$

$P_{in}$  denotes the energy of incident photon

Where  $\eta$  is the energy transfer, short circuit ( $J_{sc}$ ), picture voltage of open circuit ( $V_{oc}$ ), Fill Factor (FF) and light incident ( $P_{in}$ ).

$$FF = \frac{J_{max} \times V_{max}}{J_{sc} \times V_{oc}} \quad \text{----- (10)}$$

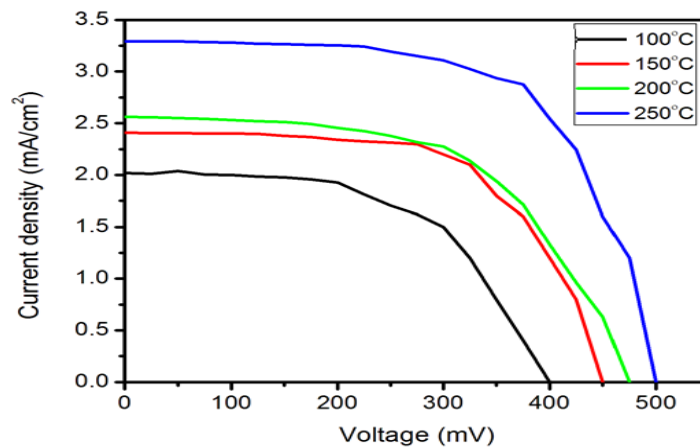


Fig (b).3.7.J-V characteristics of dye sensitized Ag thin film

**Table.3 DSSCs with electrode of Ag Films derived from the dye extracted from**

*Vitex negundo*

Substrate temperature (°C)	J <sub>sc</sub> (mA/cm <sup>2</sup> )	V <sub>oc</sub> (mV)	FF	η%
100	2.0	400	0.56	1.50
150	2.48	450	0.66	2.4
200	2.52	475	0.72	2.8
250	3.26	500	0.80	4.3

## CONCLUSIONS

It has been verified on the basis of studies that the heating temperature of the substrate in the mechanism of Pyrolysis by spray plays an important role in the deposition of thin film FTO glass plates using the system of spray pyrolysis. For the preparation of thin silver films, the substrate temperatures were optimized at 250°C respectively, for thin silver films. XRD designs of the films had orientation of the face center cubic structure centered on the face along the plane (111). The FE-SEM grains of spherical shape. EDX increased Ag nanofilm. AFM images showed an improvement surface roughness. Optimization between the morphological characteristic and the surface area of the silver film has been found to provide a significant improvement in DSSC conversion efficiency. Maximum optical absorption the film was noted for prepared in 250°C and optical band range Upgraded to 3.6 eV increased temperature of the substrate. The optical constants, like the refractive index, the extinction coefficient has shown some variations with increasing substrate temperature. Refractive index of the film prepared was slightly higher. PL emission showed the defects in the sprayed film, the increase of the substrate temperature (250 ° C). DSSCs were different substrate temperatures of Ag thin films using *Vitex negundo* as dye. The substrate temperature 250°C using dye as sensitizer based DSSC showed maximum conversion efficiency of 4.3%.

## Acknowledgment

The author is grateful toward the thank University grant Commission in New Delhi, India.

## References

1. Arunachalam A, Dhanapandian S and Manoharan C (2015). Influence of Zn source on the performance of enhanced photo catalytic and dye sensitized solar cells efficiency based TiO<sub>2</sub> films prepared by spray pyrolysis, *J.Mater Scimitar Electron*, 10179-10193.
2. Berginc M, Opara Krasovec U, and Topic M, (2014). Outdoor ageing of the dye sensitized solar cell under different operation regimes, *Solar Energy Materials and Solar Cells*, 491–499.
3. O'Regan B, Gratzal M, (1991). A low-cost, high efficiency solar cell based on dye sensitized colloidal TiO<sub>2</sub> films. *Letters of Nature*, 737–740.

4. Chang S, Li Q, Xiao X, Wong K, Y, and Chen T, (2012). Enhancement of low energy sunlight harvesting in dye-sensitized solar cells using plasmonic goldnanorods, *physical chemistry chemical physics*, 9444–9448.
5. Lim S.P, Pandikumar A, Huang N m, Lim H.N, (2014). Enhanced photovoltaic performance of silver@titania plasmonic photo anode in dye sensitized solar cells, *Royal society of chemistry*, 38111–38118.
6. Diallo A, Beye A.c, Doyle T.B, Park E, and Maaza M, (2015). Green synthesis of Co<sub>3</sub>O<sub>4</sub> nanoparticles via *Aspalathus linearis*: physical properties, *Green Chemistry Letters and Reviews*, 30–36.
7. Suhaimi S, Shahimin M, Alahmed Z.A, Chyský .J, and Reshak A, (2015). Materials for Enhanced Dye sensitized Solar Cell Performance: Electrochemical Application, *International Journal of Electrochemical Science*, 2859–2871.
8. Hammad T.M, Hejazy N.K, Strip G, and Branch G, (2011). Structural, Electrical and Optical Properties of ATO Thin Films Fabricated by Dip Coating Method, *International Nano Letters*, 123–128.
9. J.-L. Brousseau, H. Bourque, A. Tessier, and R. M. Leblanc, (1997). Electrical properties and topography of SnO<sub>2</sub> thin films prepared by reactive sputtering, *Applied Surface Science*, 351–358.
10. Paraskevi and Munkegade N, (2008). Structural and sensing properties of nanocrystalline SnO<sub>2</sub> films deposited by spray pyrolysis from a SnCl<sub>2</sub> precursor, *Applied Physics A Material Science and Processing*, 667–670.
11. Youssef S.A and Ali S, (2008). The effect of fluorine doping on optoelectronic properties of tin-dioxide (F: SnO<sub>2</sub>) thin films, *CODEN JNSMAC*, 43–50. .
12. Ray S.C, .Karanjai M.K, and Dasgupta .D, (1997). Preparation and study of doped and undoped tin dioxide films by the open air chemical vapour deposition technique, *Thin Solid Films*, 221–227.
13. Goebbert .C, Nonninger R, Aegerter M.A, and H. Schmidt, (1999). Wet chemical deposition of ATO and ITO coatings using crystalline nanoparticles redispersable in solutions, *Thin Solid Films*, 79–84.
14. Gordillo, L. C. Moreno, W. de la Cruz, and P. Teheran, (1994). Preparation and characterization of SnO<sub>2</sub> thin films deposited by spray pyrolysis from SnCl<sub>2</sub> and SnCl<sub>4</sub> precursors, *Thin Solid Films*, 61–66.
15. Dahlin Fikri, Akhmad Herman Yuwono, Nofrijon Sofyan, Tri Ariniand Latifa Hanum Lalasari (2017). The effect of substrate heating temperature upon spray pyrolysis process on the morphological and functional properties of fluorine tin oxide conducting glass, *American Institute of Physics*, 1826-1827.
16. Saravanan S, Kato R, Balamurugan M, Kaushik S, and Soga T (2017). Efficiency improvement in dye sensitized solar cells by the plasmonic effect of green synthesized silver nanoparticles, *Journal of Science: Advanced Materials and Devices*, 418-424.
17. Gordillo G, Moreno C, de la w, Cruz, and Teheran p (1994). Preparation and characterization of SnO<sub>2</sub> thin films deposited by spray pyrolysis from SnCl<sub>2</sub> and SnCl<sub>4</sub> precursors, *Thin Solid Films*, 61–66.
18. Chapala A, Kusior E, and Bucko M, (1989). Optical properties of non-stoichiometric tin oxide films obtained by reactive sputtering, *Thin Solid Films*, 15–22.
19. Arunachalam, Dhanapandiyan .S, manoharan C and Sridhar (2015). Characterization of sprayed TiO<sub>2</sub> on ITO substrates for solar cell applications, *Spectrochimica Acta part a: molecular and bimolecular spectroscopy*, 904-912.
20. Arunachalam, Dhanapandiyan .S, manoharan C and Sridhar (2015). Characterization of sprayed TiO<sub>2</sub> on ITO substrates for solar cell applications, *Spectrochimica Acta part A: molecular and bimolecular spectroscopy*, 149,904-912.
21. Rahal A, Benramache S, and Benhaoua B, (2013). The effect of the film thickness and doping content of SnO<sub>2</sub>: F thin films prepared by the ultrasonic spray method, *Journal of Semiconductors*, 93003–93004.

22. Arunachalam .A, Dhanapandiyan .S and Manoharan C **(2012)**.Influence of Zn source on the performance of enhanced photo catalytic and dye sensitized solar cells efficiency based Tio<sub>2</sub> films prepared by spray pyrolysis, *J.Matter Sci: Mater Electron* 3705-3706.
23. Zheng,J, Ding,Y, Tian .B, Wang,Z, Zhuang X, **(2008)**.Luminescent and Raman Active Silver Nanoparticles with Polycrystalline Structure, *Journal of American chemical society*, 10472–1047.
24. Shankar, Shiv S, Rai, Akhilesh ,Ahmad, Absar ,Sastry and Murali **(2004)**.Rapid synthesis of Au, Ag, and bimetallic Au core–Ag shell nanoparticles using Neem (*Azadirachta indica*) leaf broth, *Journal of Colloid Interface Science*,496–502.
25. Arshad Hussain, Ahmed R, Nisar Ali, Naser M Abdel-Salam, Karim bin Deraman and Yong Qing Fu **(2017)**.Synthesis and characterization of thermally evaporated copper bismuth Sulphide thin films, *Surface & Coatings Technology*, 404–408.
26. Zawawi .I.K, Manal A. Mahdy A.R., Yosr E.E-D. Gamal, Hisham Imam **(2107)**.Incorporation of O<sub>2</sub> with Ag/AgOx Nan composite thin films, *Super lattices and Microstructures*, 553-566.
27. Arunachalam .A, Dhanapandiyan .S, Manoharan .C, and Sridhar .R **(2015)**. Characterization of sprayed TiO<sub>2</sub> on ITO substrates for solar cell Applications, *Spectrochimica Acta Part A: Molecular and Bimolecular Spectroscopy*, 904–912.
28. Rajesh kumar B, Subba rao.T **(2012)**.Afm studies on surface morphology, topography and texture of nanostructured zinc aluminum oxide thin films, *Journal of Nanomaterials and Bio structures*, 1881-1889.
29. Jiawei Gong et al., **(2017)**.Review on dye-sensitized solar cells (DSSCs): Advanced techniques and research trends, *Renewable and Sustainable Energy Reviews* 234–246.